

# Rotation-induced phase transition in a spherical gravitating system

Peter Klinko and Bruce N. Miller

*Department of Physics and Astronomy, Texas Christian University, Fort Worth, Texas 76129*

Igor Prokhorenkov

*Department of Mathematics, Texas Christian University, Fort Worth, Texas 76129*

(Received 23 February 2001; published 29 May 2001)

Due to the infinite range and singularity of the gravitational force, it is difficult to directly apply the standard methods of statistical physics to self-gravitating systems, e.g., interstellar grains, globular clusters, galaxies, etc. Unusual phenomena can occur, such as a negative heat capacity, unbounded mass, or the gravothermal catastrophe where the equilibrium state is fully collapsed and the entropy is unbounded. Using mean field theory, we investigate the influence of rotation on a purely spherical gravitational system. Although spherical symmetry nullifies the total angular momentum, its square is finite and conserved. Here we study the case where each particle has specific angular momentum of the same magnitude  $l$ . We rigorously prove the existence of an upper bound on the entropy and a lower bound for the energy. We demonstrate that, in the microcanonical and canonical ensembles, a phase transition occurs when  $l$  falls below a critical value. We characterize the properties of each phase and construct the coexistence curve for each ensemble. Possible applications to astrophysics are considered.

DOI: 10.1103/PhysRevE.63.066131

PACS number(s): 64.60.-i, 05.20.-y

## I. INTRODUCTION

Because of the large population of some stellar systems, such as galaxies and globular clusters, it is natural to believe that maximum entropy principles should be central to their understanding. Although their populations are much smaller than those of typical galaxies, globular clusters are the system of choice for theoretical investigation because, in contrast with galaxies, their relaxation times are substantially less than the age of the universe [1,2]. Observations of their density profiles suggest that there are two varieties distinguished by the presence of a condensed core [2,3], commonly referred to as a core-halo structure. At issue is the possibility that the clusters can exist in different thermodynamic phases.

Unfortunately the role of thermodynamics and statistical physics as tools for understanding the structure and evolution of gravitational systems has not been clearly determined. Both the infinite range and short range singularities of the Newtonian interaction result in technical barriers that are difficult to overcome. These include an un-normalizable density [4] and a divergent partition function [5]. Historically the infinite range of the gravitational force, and the associated problem of escape, was dealt with by theorists by artificially confining the system in a spherical box [4,6]. Even with this restriction, the thermodynamics is not completely manageable due to the lack of a global entropy maximum at fixed mass and energy [7,8] which precludes the existence of a stable equilibrium state. A state of arbitrarily large entropy can be constructed in the isolated system by concentrating sufficient mass in the system center, a phenomenon known in the astronomy literature as the “gravothermal catastrophe” [8]. When the energy is above a critical value, however, metastable states yielding local entropy maxima are available to the system [4,8]. On the other hand, it has been rigorously proven that if the system is open to energy exchange with the

environment, the only equilibrium state is completely collapsed [5].

It is clear that for systems occurring in nature the short range singularity is artificial, e.g., real stars have finite radii that are not breached by collisions unless a cluster is very old [2]. Since the lack of an entropy bound is caused by the singularity in the force, regularizing the potential in some manner could result in radically different thermodynamics. It was first conjectured by Lynden-Bell and Wood that, if the particles possess a hard sphere core, not only should an entropy maximum exist, but a phase transition could occur as well under the appropriate conditions [8]. This was investigated by a few authors using an approximate form of mean field theory, in which a local pressure due to the short range repulsion is combined with a continuum Vlasov description [1] of a gravitational system. Employing equations of state of increasing accuracy for the local pressure [9–11], respectively, the conjecture was verified within the limitations of the approximations. At a sufficiently low energy in the microcanonical ensemble (MCE) or temperature in the canonical ensemble (CE), a transition to a more centrally concentrated phase is predicted. An open question is whether this, or a similar transition, can account for the existence of the distinct globular cluster families mentioned earlier. An alternative mean field formulation was recently carried out for a spherical system in which the effect of a different regularization, constructed by approximating the Newtonian potential as a truncated series of spherical Bessel functions, was explored directly in the Vlasov limit [12]. It will be interesting to see if a similar thermodynamics is also predicted by this model.

It is important to note that the nature of the gravitational transition differs strongly from our everyday experience with “chemical” systems characterized by short range interactions. Here there is no thermodynamic limit as such. We do not find the system in distinct, coexistent phases separated

spatially by a sharp boundary. Further, a jump in temperature occurs at the transition in the CE, and stable states with negative heat capacity exist just above the transition in the MCE. These features, and others, are elucidated in greater detail elsewhere [6,11]. They are shared with other model systems that possess a purely attractive interaction potential [13].

In order to put these ideas on firmer ground, in the last few years a model system consisting of concentric, spherical mass shells was investigated in our group using both mean field theory and dynamical simulation. The shells are irrotational, have infinitesimal thickness, and interact only through their mutual gravitational attraction, i.e., they simply pass through each other on contact. As in the earlier studies, the effective one-dimensional system (the only coordinate is the shell radius) was restricted to lie within a spherical box. In addition, the singularity was shielded by the inclusion of a hard inner barrier of, say, radius  $a$ . Preliminary stages of the investigation included a study of the ergodic properties of a pair of shells [14] and the time scale for relaxation to equilibrium [15]. Because of the simplicity of the model, it was possible to formulate the mean field theory exactly and solve the resulting nonlinear differential equation for the density profile with numerical accuracy [16,15]. It was also possible to simulate the system dynamically for long times, well beyond the time required to reach equilibrium in most situations [16,15]. The system was studied in the microcanonical and canonical ensembles, and a restricted version of the grand canonical ensemble (GCE). When the screening radius  $a$  falls below a critical value  $a_c$ , mean field theory predicts a phase transition in the MCE and CE but not in the GCE for the particular choice of average mass. It is important to note that the numerical value of  $a_c$  depends on the choice of ensemble. The simulations confirmed the theoretical predictions when the influence of finite size scaling was taken into account [17–19]. In addition to confirming the predictions of mean field theory, unanticipated information concerning both temporal and positional correlations was extracted from the simulations, which further demonstrated the difference between gravitational and chemical systems [15].

A second open question concerns the uniqueness of regularization as a mechanism for preventing the formation of a singular, collapsed, core, i.e., gravothermal catastrophe. In this work we wish to consider a different mechanism for inducing a phase transition in a gravitational system. From symmetry considerations it is clear that for a spherical system of point particles moving in three dimensions the total angular momentum vanishes. However, it is also well established that, in the mean field limit, the sum of the squares of the angular momenta of the constituent particles,  $\sum l_i^2 \equiv L_2$ , is an integral of the motion [1]. Since a particle with fixed, nonvanishing, angular momentum cannot reach the system center, it was thought that rotational effects may be able to prevent the development of a singular central density that would otherwise occur, thus preventing the gravothermal catastrophe. To investigate this possibility, recently we extended both the microcanonical and canonical ensembles to include the second integral [19]. We examined both rotating shell systems of differing dimension (without the inner bar-

rier constraint), and a three-dimensional system consisting of point particles, all in the mean field limit. It is surprising that the gravothermal catastrophe was still possible in each ensemble. Apparently fixing  $L_2$  or its average is not sufficient to prevent mass from reaching the system center.

In the present work we go one step further; i.e., we endow each particle or shell with a fixed value of the square of the angular momentum,  $l^2$ . This establishes a centrifugal barrier in the system which resists collapse. In the following we first define the system. We then use mean field (Vlasov) theory to formulate the system thermodynamics and derive a differential equation for the local gravitational potential energy. This, in turn, is used to obtain the local system density. We then prove unequivocally that, for  $l^2 \neq 0$ , a lower bound for the energy and upper bound for the entropy always exist. Next we investigate the system behavior in the MCE and CE for different values of  $l^2$  and energy or, respectively, temperature, by employing numerical integration. We show that below a critical value, say  $l_c^2$ , a phase transition is possible in both the CE and MCE, where here as well the numerical value of  $l_c^2$  depends on the choice of ensemble, and we investigate the system behavior in each phase. In the Conclusion we will discuss how this simple model, and some extensions, may have astrophysical significance.

## II. FORMULATION OF THE MODEL

The mean field (or Vlasov) limit is constructed from the regular Hamiltonian system of  $N$  particles, mass  $M$ , and energy  $E$ , by taking the constrained limit  $N \rightarrow \infty$ , with  $M$  and  $E$  held constant. The system is then uniquely and completely described by the single-particle distribution function in position and velocity,  $f(\mathbf{r}, \mathbf{v}, t)$  [1,20]. For our model system of concentric, infinitesimal, rotating mass shells, each shell is assigned the same magnitude of angular momentum per unit mass,  $l$ , in units where the moment of inertia is  $mr^2$ . Ignoring any internal coordinates, the radial motion of each shell is fully characterized by  $r$ ,  $v$ , and  $l$ , where  $r$  is the radial coordinate and  $v$  is the radial velocity. Thus, in the mean field limit, the stationary system is completely described by the probability density function  $f(r, v)$ . The system is confined in a spherical box with  $r \leq b$ . For convenience we employ units where  $M = G = b = 1.0$  where, as usual,  $G$  is the universal gravitational constant.

Let us consider a confined system in the mean field limit with the following Hamiltonian density:

$$H = \frac{1}{2}v^2 + \frac{l^2}{2r^2} + \Phi(r),$$

where the gravitational potential  $\Phi$  is a solution of the Poisson equation, and  $l^2$  is a constant. We can think of several types of spherical system for which the radial motion is represented by the above Hamiltonian. For example, the three-dimensional point mass system with fixed magnitude of the angular momentum has the same Hamiltonian per unit mass. Alternatively, we can think of a system of infinitesimally thin rotating shells if we fix the magnitude of each shell's angular momentum. We can derive the thermodynamics of

this family in the mean field limit. We will show that an extremum for the entropy is realized when  $f \propto \exp(-\beta H)$ . This model is a special case of the more general problem of spherically symmetric, self-gravitating systems [19], but here  $l^2$  is independently fixed for each particle. This latter condition also ensures that the system energy is bounded from below for any  $l^2$ . We will show that the minimum energy configuration is realized physically when the mass is at rest and concentrated at a unique radius.

### A. Entropy bound

In this section we prove the existence of an upper bound on entropy  $S[f]$ , where the density  $f$  is assumed to satisfy the constraints of normalization and mean total energy. This bound depends on the energy  $E$  and angular momentum magnitude  $l$ . As a part of our proof we estimate the mean potential energy from below in terms of  $l$ . In the next section we calculate critical values of the entropy functional and investigate their stability. First we will show that there is a unique  $f(r, v)$  that provides an extremum for the entropy  $S[f]$  with respect to the constraints of normalization and the mean total energy:

$$\int \int f dv dr = 1, \quad (1)$$

$$\int \int f \left( \frac{1}{2} v^2 + \frac{l^2}{2r^2} + \frac{\Phi}{2} \right) dv dr = E, \quad (2)$$

where, in mean field theory,  $S$  takes the form [1,6]

$$S = - \int \int f \ln f dv dr \quad (3)$$

in units where  $k_B$ , the Boltzmann constant, is unity. In the above it is implicitly assumed that the integration over radial velocity is over the whole real line, while the integration over position is restricted to the unit interval. For convenience, unless otherwise indicated, we will adhere to this convention throughout the remainder of the paper.

From the standard variational treatment [18] we know that  $f(r, v)$  takes the form

$$f(r, v) = C \exp \left[ -\beta \left( \frac{1}{2} v^2 + \frac{l^2}{2r^2} + \Phi \right) \right], \quad (4)$$

where  $\alpha$  and  $\beta$  are the Lagrange multipliers, and  $C = \exp[-(\alpha+1)]$ . The probability density function, which is identical to the linear mass density function in our system of units, is then

$$\rho(r) = \int f dv = A \exp \left( -\beta \frac{l^2}{2r^2} - \beta \Phi \right), \quad (5)$$

where  $A = C \sqrt{2\pi/\beta}$ .

We start by studying the following variational problem for the entropy  $S$ :

$$S[f] \rightarrow \text{extr},$$

subject to two constraints,

$$\int f(r, v) dv = \rho(r)$$

and

$$\frac{1}{2} \int \int v^2 f(r, v) dv dr = K.$$

Here  $\rho(r)$  denotes fixed density (after the velocity dependence is integrated out) and  $K$  denotes the kinetic energy. After introducing two Lagrange multipliers  $\lambda(r)$  and  $\beta$ , we have

$$\delta \left( S[f] - \int_0^1 \lambda(r) \rho(r) dr - \beta K \right) = 0,$$

or

$$\int \int [-1 - \ln f - \lambda(r) - \frac{1}{2} \beta v^2] \delta f dv dr = 0.$$

Therefore, extremal solutions  $\varphi(r, v)$  to this variational problem have Gaussian distributions in velocity:

$$\varphi(r, v) = e^{-1 - \lambda(r) - \beta v^2/2}.$$

From the two constraints above we have

$$\varphi(r, v) = \sqrt{\beta/2\pi} e^{-\beta v^2/2} \rho(r),$$

and, if we normalize,  $\int \rho(r) dr = 1$ ,

$$K = \frac{1}{2\beta}. \quad (6)$$

It is easy to show that this extremal solution is the maximum; that is, for all  $f(r, v)$  satisfying the constraints above we have

$$S[f] \leq S[\varphi].$$

Indeed, consider a one-parameter family of density functions  $f_t = \varphi + th$ , with  $f_0(r, v) = \varphi(r, v)$  and  $f_1(r, v) = f(r, v)$ . If

$$\int h(r, v) dv = \int v^2 h(r, v) dv = 0,$$

then for all  $0 \leq t \leq 1$  functions  $f_t(r, v)$  will satisfy the same constraints as  $f(r, v)$ . Define

$$F(t) = S[f_t] - S[f].$$

Since  $F(0) = 0$ ,  $F'(0) = 0$ , and  $F''(t) \leq 0$  for all  $0 \leq t \leq 1$ ,  $F(t)$  is a decreasing function of  $t$  and  $F(t) \leq 0$ . Thus the inequality  $S(f) \leq S(\varphi)$  is proved.

Next we study the conditions satisfied by the density  $\rho(r)$  that provides an extremum for the entropy of the system subject to the constraints of normalization, Eq. (1), and of the total potential energy  $\Pi$ . We have shown that  $f$  is of the form

$$f(r, v) = \sqrt{\beta/2\pi} e^{-\beta v^2/2} \rho(r),$$

then, after integrating  $v$  out and asserting Eq. (6) we obtain two constraints on  $\rho(r)$ :

$$\begin{aligned} \int \rho(r) dr &= 1, \\ \int \rho \left( \frac{l^2}{2r^2} + \frac{\Phi}{2} \right) dr &= \Pi. \end{aligned} \quad (7)$$

The gravitational potential  $\Phi(r)$  can be expressed in terms of the density from the solution of the Poisson equation for a spherical mass distribution. This is usually written in the form

$$\Delta \Phi(r) = 4\pi G \rho_v(r)$$

where  $\rho_v(r)$  is the mass density per unit volume. Since our system is effectively one dimensional, here and in Eq. (5),  $\rho(r) = 4\pi r^2 \rho_v(r)$  is the linear mass density and the Laplace equation takes the form

$$\frac{d}{dr} r^2 \frac{d}{dr} \Phi(r) = \rho(r). \quad (8)$$

For simplicity, we select the solution that vanishes at infinity and, therefore, satisfies the boundary condition  $\Phi(b) = -MG/b$ , so that, in our units,

$$\Phi(r) = -\frac{1}{r} \int_0^r \rho(z) dz - \int_r^1 \frac{\rho(z)}{z} dz. \quad (9)$$

Now, from Eqs. (3) and (4),

$$\begin{aligned} S[f] &= - \int [\sqrt{\beta/2\pi} e^{-\beta v^2/2} \rho(r)] \\ &\quad \times \ln[\sqrt{\beta/2\pi} e^{-\beta v^2/2} \rho(r)] dv dr \\ &= - \int \rho(r) \ln \rho(r) dr - \ln \sqrt{\beta/2\pi} + \frac{1}{2}. \end{aligned} \quad (10)$$

Our goal is to bound the entropy from above in terms of fixed  $E$  and  $l$ . Since for any positive function  $\rho(r)$  we have

$$- \int_0^1 \rho(r) \ln \rho(r) dr \leq \max(-z \ln z) \leq \frac{1}{e},$$

it is enough to bound the value of  $\ln 1/\beta$  from above, because

$$S[f] \leq C' + \frac{1}{2} \ln \frac{1}{\beta},$$

where

$$C' = \frac{1}{e} + \frac{1}{2} \ln 2\pi + \frac{1}{2}.$$

## B. Energy bound

An essential step in bounding  $\ln 1/\beta$  is to find a lower bound on  $\Pi$ , the total, mechanical potential energy of our system, in terms of fixed  $l$ . From the formula for  $\Phi(r)$ ,

$$\Phi(r) \geq -\frac{1}{r} \int_0^r \rho(z) dz - \frac{1}{r} \int_r^1 \rho(z) dz = -\frac{1}{r}.$$

Therefore,

$$\Pi = \int \rho \left( \frac{l^2}{2r^2} + \frac{\Phi}{2} \right) dr \geq \int \rho \left( \frac{l^2}{2r^2} - \frac{1}{2r} \right) dr.$$

On the interval  $[0, 1]$  the function  $g(r) \equiv l^2/2r^2 - 1/2r$  has a minimum  $g(2l^2) = -1/8l^2$  if  $0 \leq l \leq \sqrt{2}/2$ , and  $g(1) = (l^2 - 1)/2$  if  $l > \sqrt{2}/2$ . Therefore,

$$\Pi \geq \begin{cases} -\frac{1}{8l^2} & \text{if } 0 \leq l \leq \frac{\sqrt{2}}{2} \\ \frac{l^2 - 1}{2} & \text{if } l > \frac{\sqrt{2}}{2}. \end{cases}$$

Note that the equalities in the estimates are achieved when  $\rho(r)$  is a  $\delta$  function centered, respectively, at  $r = 2l^2$  and  $r = 1$ . Thus the estimates are exact. Since kinetic energy is always non-negative, these estimates also serve to bound the total energy of the system from below in the mean field limit.

Since

$$E = \frac{1}{2\beta} + \Pi, \quad (11)$$

it is easy to obtain the following estimates:

$$\ln \frac{1}{\beta} \leq \begin{cases} \ln \left( 2E + \frac{1}{4l^2} \right) & \text{if } 0 \leq l \leq \frac{\sqrt{2}}{2} \\ \ln(2E + 1 - l^2) & \text{if } l > \frac{\sqrt{2}}{2}. \end{cases}$$

Finally we have the following bounds for the entropy:

$$S(f(r, v)) \leq \begin{cases} C' + \frac{1}{2} \ln \left( 2E + \frac{1}{4l^2} \right) & \text{if } 0 \leq l \leq \frac{\sqrt{2}}{2} \\ C' + \frac{1}{2} \ln(2E + 1 - l^2) & \text{if } l > \frac{\sqrt{2}}{2}. \end{cases}$$

Thus, for this system, gravothermal catastrophe is not possible.

## III. DIFFERENTIAL EQUATION FOR THE DENSITY

All of the important thermodynamic functions can be expressed in terms of the temperature and density. Therefore, to investigate the system properties, it is essential to determine the local density  $\rho(r)$  with numerical precision. The Poisson equation (8) provides a second order differential equation for the gravitational potential which, along with Eq. (5), becomes

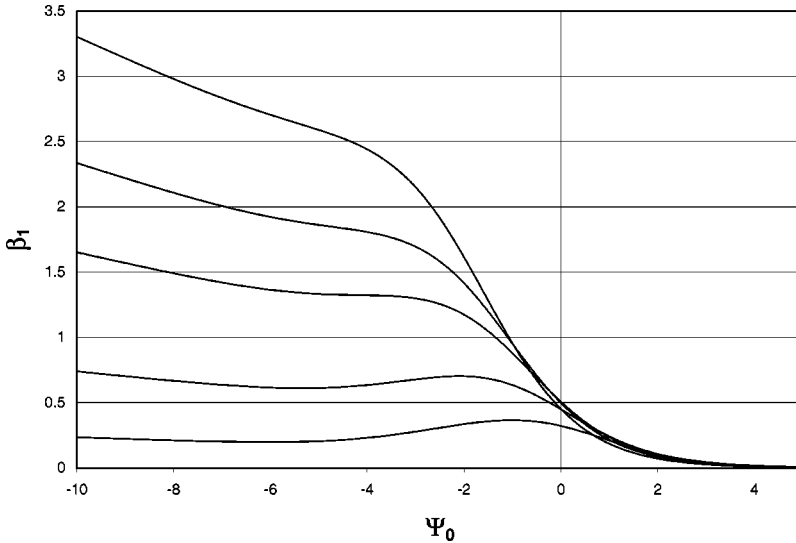


FIG. 1.  $\beta_1$  vs  $\Psi_0$  for different values of  $\beta$  when  $l^2=0.1$ .  $\beta=2.0,1.0,0.5,0.1,0.01$  (from top to bottom) in our dimensionless units. As we can see, multiple solutions are possible for  $\beta_1(\Psi_0) - \beta=0$ .

$$\frac{d}{dr} \left( r^2 \frac{d\Phi}{dr} \right) = A \exp \left( -\beta \frac{l^2}{2r^2} - \beta\Phi \right)$$

or, in a more convenient form,

$$\frac{d}{dr} \left( r^2 \frac{d\Psi}{dr} \right) = A' \exp \left( -\beta \frac{l^2}{2r^2} - \Psi \right), \quad (12)$$

where  $A' = A\beta$  and  $\Psi = \beta\Phi$ . Once the scaled gravitational potential  $\Psi$  is known, it is easy to construct the density from Eq. (5). From symmetry and consistency with our definition of the potential, we have to solve Eq. (12) with the boundary conditions  $\Psi'(0) \equiv d\Psi/dr|_{r=0} = 0$  and  $\Psi(1) = -\beta$ . Thus, at first glance, Eq. (12) looks like an ordinary, nonlinear, second order differential equation with conditions specified on each boundary of the unit interval. However, there is a further complicating feature brought about because the density must be properly normalized. It is easy to see that this imposes the following condition on  $A'$  and hence  $\Psi$ :

$$A' \int_0^1 \exp \left( -\beta \frac{l^2}{2r^2} - \Psi \right) dr = \beta = \frac{d\Psi}{dr} \Big|_{r=1}.$$

Thus  $A'$  is a functional of  $\Psi$ . We will solve Eq. (12) with the following approach. First we will relax the conditions on  $\Psi(1)$  and  $A'$  [or, equivalently,  $\Psi'(1)$ ]; then we will convert Eq. (12) to an initial value problem, integrate it numerically, and, finally, reassert the conditions.

Notice that we can always add a constant to  $\Psi$  without changing the physics. This will not alter the value of the density or entropy, but will shift the total energy by a constant. Therefore, with no loss of generality, we are free to choose the initial value  $\Psi_0 = \Psi(0)$  such that the normalization constant for the density [see Eq. (5)]  $A = 1/\beta$ , and [see Eq. (12)]  $A' = 1$ . Then, with this convention, and defining  $\beta l^2/2 \equiv \gamma$ , it is straightforward to show that the second order equation (12) can be converted to the following system of coupled, first order equations,

$$\frac{dy}{dr} = \exp(-\Psi - \gamma/r^2),$$

$$\frac{d\Psi}{dr} = \frac{y}{r^2}. \quad (13)$$

In practice, we use numerical integration to solve the initial value problem in this form [Eq. (13)] with

$$\Psi'(0) = 0,$$

$$\Psi(0) = \Psi_0.$$

However the initial value problem above is not equivalent to the original problem because there we have the additional condition  $y(1) = \beta$  arising from the normalization of  $\rho$ . For arbitrary  $\Psi_0$ ,

$$\int_0^1 \exp(-\Psi - \gamma/r^2) dr \equiv \beta_1(\Psi_0, \gamma), \quad (14)$$

which means that

$$y(1) = \beta_1(\Psi_0, \gamma).$$

Thus, constructing those solutions that satisfy the condition  $y(1) = \beta$  is equivalent to finding  $\Psi_0$  such that  $\beta_1(\Psi_0, \gamma) - \beta = 0$  for a given  $\gamma, \beta$  or, alternatively,  $l^2, \beta$  pair.

In practice, we numerically integrated the coupled equations (13), using the Bulirsch-Stoer algorithm [21] for different values of  $\Psi_0$  and  $\gamma$ . In Fig. 1, we present plots of  $\beta_1(\Psi_0, \gamma)$  versus  $\Psi_0$  for a family of fixed values of  $\gamma$ . We can see from the figure that there is a critical value of  $\gamma$ , say  $\gamma_c$ , such that, when  $0 < \gamma < \gamma_c$ , the curves intersect straight horizontal lines of fixed  $\beta_1 = \beta$  in three points, demonstrating the existence of multiple solutions. In the next section we will see how they allow the physical system to exist in different thermodynamic phases.

In addition to numerically integrating the differential equations and solving for  $\Psi_0$ , in order to uniquely fix  $E$  and

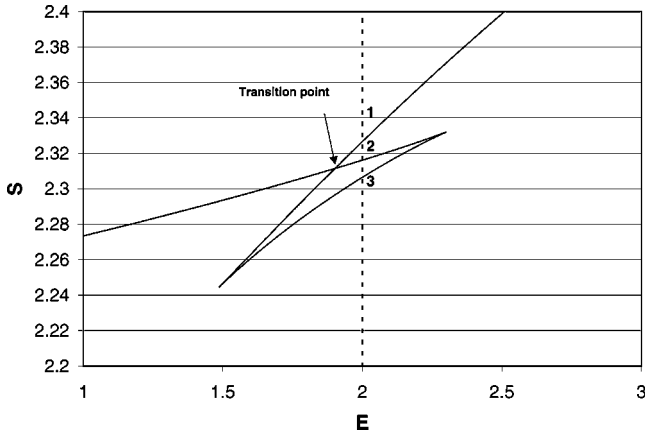


FIG. 2. Entropy vs energy (for a unit mass). The plot shows the presence of a microcanonical phase transition at  $E=1.9$  when  $l^2 = 5.0 \times 10^{-5}$  in our dimensionless units. In fact, the phase transition is present in the MCE between a condensed phase, characteristic of low energy, and a less condensed phase, characteristic of high energy, when  $l^2$  is less than the critical value  $l_c^2 = 1.1 \times 10^{-4}$  (see also Fig. 8 below). We also labeled the three distinct solutions above the transition point for  $E=2.0$ . Solution 1 is stable while, from Poincaré's linear series of equilibria, 2 and 3 are, respectively, locally stable and unstable points.

For  $F$  we must determine  $\Psi_c$ , the shift in  $\Psi$  that returns us to the boundary condition of the original problem. Let  $\Psi_1(r)$  denote the desired potential function that satisfies the original problem with boundary condition  $\Psi_1(1) = -\beta$ . Although  $\Psi(r)$  is the solution for the initial value problem (13) mentioned above [now assuming  $y(1) = \beta$ ], it does not necessarily satisfy the same boundary condition as  $\Psi_1(r)$ . Clearly we regain the original with

$$\Psi_1(r) = \Psi(r) - \Psi(1) + \Psi_1(1) = \Psi(r) - \Psi(1) - \beta,$$

where  $\Psi(1)$  is obtained from the numerical integration.

For the purpose of numerical evaluation, we also need to rewrite the equations for the entropy and energy in terms of the solution of the initial value problem,  $\Psi$ . Since adding a constant to the potential shifts the energy per unit mass, but has no effect on the entropy, from Eqs. (5), (10), (7), and (11) we easily find

$$S = \ln \sqrt{2\pi\beta} + \frac{1}{2} + \beta \int \frac{l^2}{2r^2} \rho dr + \int \Psi \rho dr,$$

$$E = \frac{(1 - \Psi_c)}{2\beta} + \frac{1}{2} \int \frac{l^2}{r^2} \rho dr + \frac{1}{2\beta} \int \Psi \rho dr,$$

where  $\Psi_c = \Psi(1) + \beta$  is the shift in the scaled gravitational potential. Note that these forms allow us to perform the integrations on the fly, i.e., we can carry them out while we actually numerically integrate the differential equations, and correct those terms that contain  $\Psi_c$  and  $\beta$  later. Once we have the energy and entropy, it is simple to obtain the Helmholtz free energy from  $F = E - S/\beta$ .

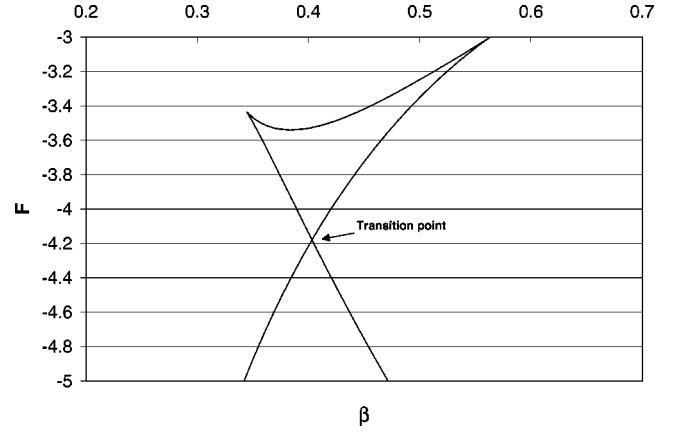


FIG. 3. Free energy vs  $\beta$  (for a unit mass). The plot shows the presence of a canonical phase transition at  $\beta=0.4$  when  $l^2 = 9.0 \times 10^{-3}$ . A phase transition is present in the CE when the parameter  $l^2$  is below the critical value  $l_c^2 = 0.025$ . Note that the value of  $l_c^2$  in the MCE is much smaller than in the CE.

#### IV. NUMERICAL RESULTS

We have shown above that for a restricted range of a single parameter,  $0 < \gamma < \gamma_c$ , multiple density profiles can occur in the system for a single  $\beta, l^2$  pair. Corresponding to  $\gamma_c$ , in each ensemble there is a critical value of  $l^2$  below which the system can exist in multiple states. To see how this translates into a phase transition in different ensembles, we examine the dependence of the entropy on the energy,  $S = S(E)$  (microcanonical ensemble) and the free energy on the inverse temperature,  $F = F(\beta)$  (canonical ensemble) for fixed values of the squared angular momentum. We find that in each ensemble there is a corresponding range of  $l^2$  where multiple thermodynamic states have the same entropy (MCE) or free energy (CE). This is seen clearly in Figs. 2 (MCE) and 3 (CE). In the isolated system (MCE) the state

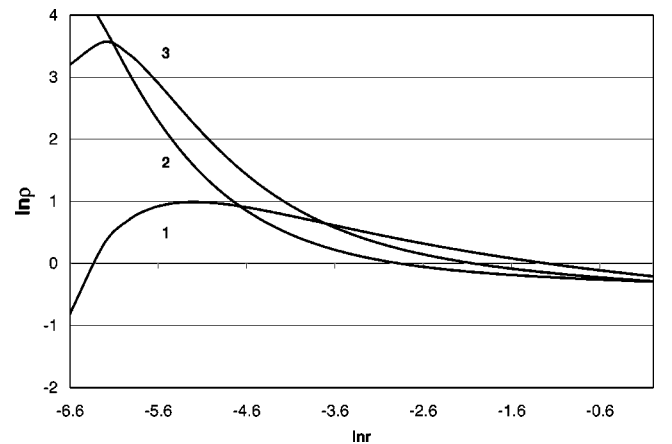


FIG. 4. The linear density profiles of the three distinct solutions labeled in Fig. 2 when  $E=2.0$  and  $l^2 = 5.0 \times 10^{-5}$ . We see that above the transition point the least condensed solution 1 is stable while solution 2 is the most condensed (corresponding to the low energy phase) and is metastable above the transition point. Solution 3 is unstable. Note that the linear density must be zero in the system center ( $r=0$ ).

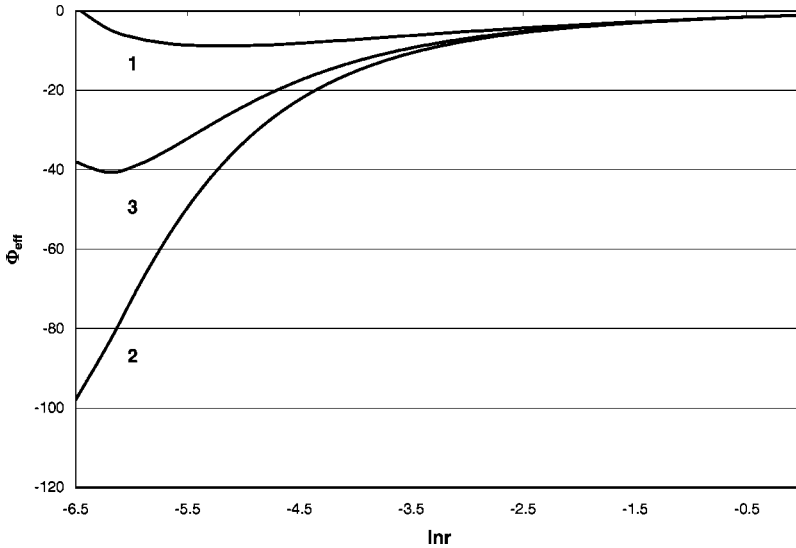


FIG. 5. The effective potential for the three distinct solutions when  $E=2.0$  and  $l^2 = 5.0 \times 10^{-5}$  (see Figs. 2 and 4). The effective potential profiles are consistent with the corresponding density profiles in Fig. 4. Since  $l^2$  is fixed and solution 1 is less condensed, its minimum in  $\Phi_{\text{eff}}$  is the farthest from the center, while solution 3's minimum of  $\Phi_{\text{eff}}$  is the closest to the center.

with maximum entropy is most stable and there is a jump in the derivative  $\partial S/\partial E = \beta$  at the transition point, while in the open system (CE) the state of minimum free energy is most stable and there is a jump in  $\partial(\beta F)/\partial\beta = E$ . Thus the transition is first order in each case. Where three phases are present, the stability of each phase can be checked using the technique known as Poincaré's linear series of equilibria [22,23,19]. This method provides a powerful tool for determining if the extremal solutions are locally stable in the appropriate function space. We applied it to confirm that, when multiple phases are present, the usual thermodynamic description is valid; i.e., there is a globally stable phase (maximum entropy in the MCE or minimum free energy in the CE), a metastable or locally stable, phase (minimum entropy or maximum free energy), and an unstable phase.

In Figs. 4 and 5 we compare the density profile  $\rho(r)$  and the effective potential  $\Phi_{\text{eff}} \equiv l^2/2r + \Phi$  for each phase at a point in the  $(E, l^2) = (2.0, 5.0 \times 10^{-5})$  parameter space of the MCE. In each case we chose  $\ln r$  for the abscissa in order to easily resolve the different structures. The points are labeled 1, 2, and 3 in Fig. 2 and represent an energy value just above the transition point. Note that the curve labeled 1 is the high energy stable phase, 2 has lower energy and is metastable, and 3 is unstable. Each density profile is peaked at a different value of  $r$ , say  $r_m$ . In Fig. 4 we see that the density profile of the low energy metastable phase 2 is most strongly peaked at the smallest value of  $r_m$  (not visible in the figure because of the choice of scale—see above) and the high energy stable phase has the smallest peak at the largest value. Although the unstable phase has the lowest energy, its structure is intermediate between the others. As a result of Eq. (5) there is a natural correspondence between the behavior of  $\rho(r)$  and  $\Phi_{\text{eff}}(r)$  which we observe in Fig. 5.

We proved in Sec. II that, for given  $l^2$ , there is a lower bound on the energy. For the case where  $l^2 < 0.5$ , the minimum potential energy is  $-1/8l^2$ . In the state of minimum energy discussed in Sec. II, mean field theory predicts that all of the mass is located at  $r_m$ , the location of the minimum of  $\Phi_{\text{eff}}(r)$ , and  $\rho(r) = \delta(r - r_m)$ . The minimum energy was verified in the numerical solutions. We found a lower bound-

ary in the energy of extremal entropy solutions numerically, and this lower bound is close to  $-1/8l^2$ .

In equilibrium theory, the location of the phase transition is determined from information concerning a single phase via the Maxwell equal area construction [17]. Using our numerical solution for the local density, we are able to follow the “motion” of the system in the  $(\beta, E)$  plane in the MCE and in the  $(S, T = \beta^{-1})$  plane in the CE for a fixed value of  $l^2 < l_c^2$ . From Figs. 6 and 7, we can determine if Maxwell's equal area condition holds around the transition point. In the MCE, we know that [17]

$$\Delta S = \int_{ABCDE} \beta dE$$

if the volume is fixed (the Boltzmann constant  $k=1$  in our system of units). Therefore, if we start and end our integration at the transition point the integral for the net change of the entropy should vanish according to Fig. 4. Now, if we look at Fig. 6 and evaluate the integral by breaking it up into

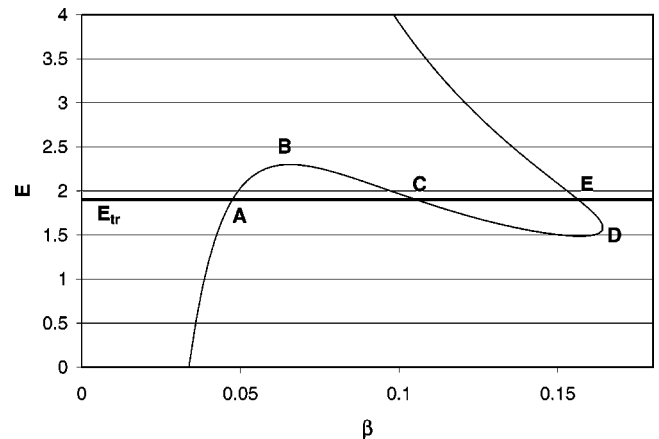


FIG. 6. Plot of energy vs inverse temperature when  $l^2 = 5.0 \times 10^{-5}$ . The transition point obtained from the Maxwell equal area construction is the same as that in Fig. 2.

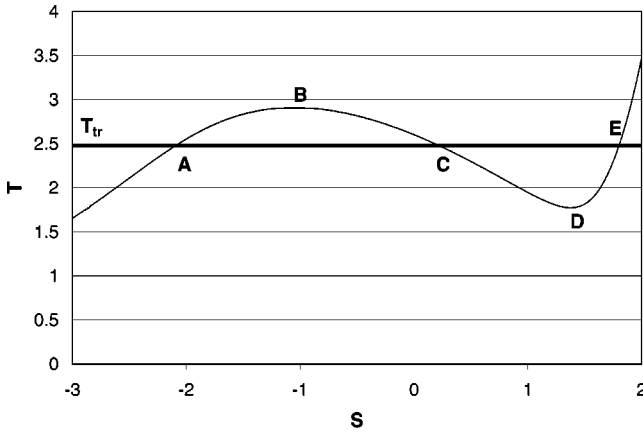


FIG. 7. Plot of temperature vs entropy when  $l^2=9.0 \times 10^{-3}$ . The transition point obtained from the Maxwell equal area construction is the same as that in Fig. 3.

four parts according to the figure, we see that the areas of  $ABC$  and  $CDE$  are equal. For the canonical case (Fig. 3),

$$\Delta F = - \int_{ABCDE} S dT.$$

If  $A$  and  $B$  are at the transition point, the net change of the free energy is zero along the path  $ABCD$ . Similarly, if we evaluate this integral by breaking it into four pieces (Fig. 7), we can see that the areas of  $ABC$  and  $CDE$  should be equal. We can determine the transition energy  $E_{tr}$  for the MCE and the transition temperature  $T_{tr}$  for the CE by inspecting the plots of  $S(E)$  (Fig. 2) and  $F(\beta)$  (Fig. 3), and we were able to numerically verify the equal area relation for each ensemble with high accuracy.

In Figs. 8 and 9, we present the phase diagrams of the system in the MCE and the CE. In each case, there are three distinct regions corresponding to a condensed phase, a quasiuniform phase, and a fluidlike phase when  $l^2 > l_c^2$ . We also indicate the regions where a metastable phase exists according to Figs. 2 and 3. As we mentioned earlier, the critical value of  $l_c^2$  is different in each ensemble, in fact  $l_{CE}^2 > l_{MCE}^2$ .

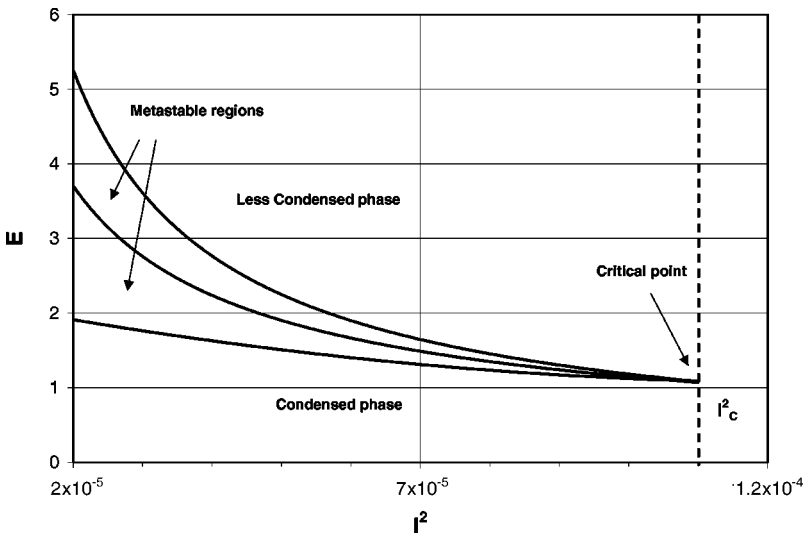


FIG. 8. Phase diagram for the MCE. The coexistence curve between the two stable phases is in the middle. The system is in the less condensed phase above the transition curve, and more condensed below it. The lines above and below the transition curve define the region where metastable solutions also exist (see Fig. 2) When  $l^2 > l_c^2$  only one phase is present.

Note that, in contrast with the canonical ensemble, in the MCE the phase transition region is in the positive energy range.

V. CONCLUSION

In earlier work [16], we showed that gravothermal catastrophe can be prevented in a shell system by the introduction of an inner reflecting barrier. However, in the more general description of three-dimensional self-gravitating systems [15], in which either  $L_2$ , the sum of the squares of the angular momentum, or its mean was fixed, we showed that gravothermal catastrophe is still present. The centrifugal barrier was not sufficient to prevent collapse. Here we were able to present a model that does not require modifying the Newtonian potential or imposing an inner boundary in order to ensure the existence of a global maximum of the entropy. The model is a simplified version of the general problem, in which the magnitude of the angular momentum is assigned the same value for each particle. In the mean field limit, the existence of an upper bound of the entropy and an energy minimum was rigorously proved, and the thermodynamics of the system was developed in both the microcanonical and canonical ensembles. In each ensemble the system undergoes a first order phase transition if  $l$  is below a critical value. This corresponds to the critical point, and the critical value of  $l$  is shown to be different in each ensemble. Plots of entropy versus energy (Fig. 2) and free energy versus inverse temperature (Fig. 3) clearly show the presence of multiple phases, one of which is stable. Applying the method of Poincaré’s linear series of equilibria, it turns out that, of the remaining solutions, one of them is a saddle point, while the other is locally stable.

We also constructed coexistence curves for both the CE and MCE, which show the conditions for each phase to exist in terms of the parameter  $l^2$  and  $E$  (MCE) or  $F$  (CE). Note that we cannot see phase transitions for negative energies in the MCE. In this ensemble the low energy phase is more centrally condensed (however, note that the density function is always zero in the center). Similar considerations apply to the canonical ensemble, where the low temperature phase is



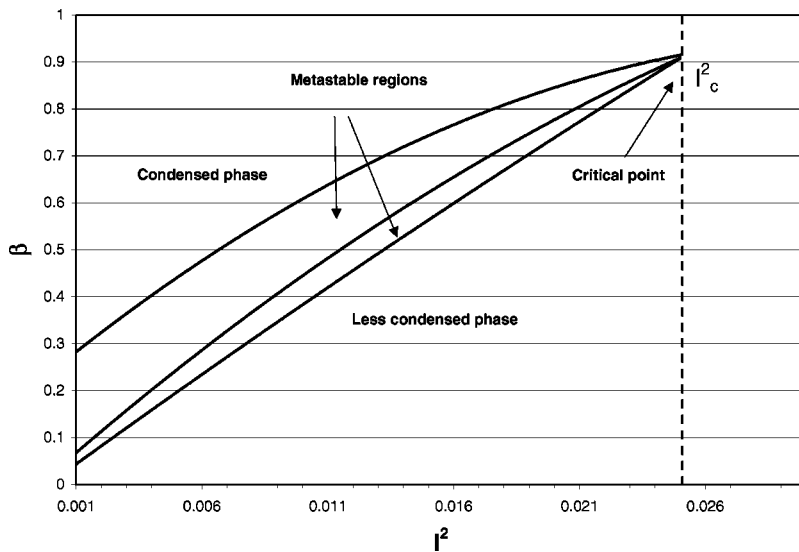


FIG. 9. Phase diagram for the CE. The middle line corresponds to the transition point, and the high temperature phase is the less condensed phase. When  $l^2 > l_c^2$  only one phase is present. The lines above and below the transition line define the region of metastable solutions (see Fig. 3).

more centrally condensed. The conditions where the energy has a minimum were also investigated numerically and it was found that the mass distribution was strongly localized within the accuracy of our code. Of course we cannot obtain the  $\delta$  function as the numerical solution of a differential equation. We rigorously proved in Sec. II that the energy is bounded from below, and this energy minimum represents the case where all the particles have vanishing radial velocity components and are concentrated in a shell with radius  $r = 2l^2$  (in our system of units) if  $l < \sqrt{2}$  and  $r = 1$  (the outer boundary) otherwise. The latter result also justifies the claim that if we fix the magnitude of the angular momentum we have a lower bound in the energy and an upper bound for the entropy which eventually prevents the gravothermal catastrophe. This model system is an outgrowth of our previous work and clearly illustrates how the thermodynamics of a spherical self-gravitating system is influenced by the manner in which angular momentum is distributed among the constituent particles.

Starting with the original conjecture of Lynden-Bell and Wood [8], all of the gravitational phase transitions studied to date concern highly idealized systems. All of them involve some type of confining outer boundary. In addition, some require removal of the short range singularity by a hard (or soft) sphere or, in the case considered here, an artificial constraint on the angular momentum of each body. Thus it is difficult to argue from a position of strength that any of these models have astrophysical relevance. Probably the most convincing case for applicability was made by Stahl *et al.* [11] for applicability to planet or asteroid formation. In future work it may be possible to relate the outer boundary to the

region in which a globular cluster blends into the background density of the parent galaxy. The effective size of this region will no doubt be influenced by dynamical processes, such as the periodic traversal of the galactic disk [2]. The case for fixed angular momentum is even harder to justify, but the contrast with the previously studied ensembles in which only the total value of  $L_2$  is constrained, either exactly or in the mean [19], may be insightful. It suggests that, under circumstances where there is a separation of time scales such that energy exchange among particles is nearly complete, but angular momentum exchange has hardly occurred, the discussion provided here may have relevance. Of course, the assumption that all angular momenta are equal, or approximately equal, is highly unlikely, but it may roughly describe the “precollapsed” state of a globular cluster [2]. What we have shown here is that if  $L_2$  mixing has not occurred the existence of distinct thermodynamic phases seems likely. However, the alternative situation where low angular momentum stars have collapsed to form a dense core while stars with nonzero angular momentum persist for long times in a diffuse halo may represent the approximate equilibrium configuration of a “postcollapse” cluster. In future work we plan to investigate the thermodynamics of this situation, as well as carry out accurate dynamical simulations of rotating shell systems to investigate the relevant relaxation processes.

#### ACKNOWLEDGMENTS

The authors are grateful for the support of the Research Foundation and the Department of Information Services of Texas Christian University.

- [1] J. Binney and S. Tremaine, *Galactic Dynamics* (Princeton University Press, Princeton, NJ, 1987).
- [2] D. C. Heggie and G. Meylan, *Astron. Astrophys. Rev.* **8**, 1 (1997).
- [3] J. E. Gunn and R. F. Griffin, *Astron. J.* **84**, 752 (1979).

- [4] S. Chandrasekhar, *An Introduction to the Theory of Stellar Structure* (Dover, New York, 1939).
- [5] M. K. Kiessling, *J. Stat. Phys.* **55**, 203 (1989).
- [6] T. Padmanabhan, *Phys. Rep.* **188**, 285 (1990).
- [7] V. A. Antonov, in *Dynamics of Star Clusters*, edited by J.

- Goodman and P. Hut, IAU Symposium No. 113 (Dordrecht, Reidel, 1985), pp. 525-540.
- [8] D. Lynden-Bell and R. Wood, *Mon. Not. R. Astron. Soc.* **138**, 495 (1968).
- [9] E. B. Aronson and C. J. Hansen, *Astrophys. J.* **177**, 145 (1972).
- [10] T. Padmanabhan, *Astrophys. J., Suppl. Ser.* **71**, 651 (1989).
- [11] B. Stahl, M. K.-H. Kiessling, and K. Schindler, *Planet. Space Sci.* **43**, 271 (1995).
- [12] E. Follana and V. Lalieta, *Phys. Rev. E* **61**, 6270 (2000).
- [13] P. Hertel and W. Thirring, *Ann. Phys. (N.Y.)* **63**, 520 (1971).
- [14] B. N. Miller and P. Youngkins, *Chaos* **7**, 187 (1997).
- [15] P. Youngkins and B. N. Miller, *Phys. Rev. E* **56**, R4963 (1997).
- [16] B. N. Miller and P. Youngkins, *Phys. Rev. Lett.* **81**, 4794 (1997).
- [17] P. Youngkins and B.N. Miller, *Phys. Rev. E* **62**, 4883 (2000).
- [18] R. K. Pathria, *Statistical Mechanics*, 2nd ed. (Butterworth-Heinemann, London, 1996).
- [19] K. Binder, *Ferroelectrics* **73**, 43 (1987).
- [20] P. J. Klinko and B. N. Miller, *Phys. Rev. E* **62**, 5783 (2000).
- [21] W. Braun and K. Hepp, *Commun. Math. Phys.* **56**, 101 (1977).
- [22] W. H. Press, S. A. Teukolsky, B. P. Flannery, and W. T. Vetterling, *Numerical Recipes in C* (Cambridge University Press, Cambridge, 1988).
- [23] J. Katz, *Mon. Not. R. Astron. Soc.* **183**, 765 (1978).
- [24] J. Katz, *Mon. Not. R. Astron. Soc.* **189**, 817 (1979).